Synthesis, X-Ray Characterization and Molecular Structure of a Novel Supramolecular Compound of Antimony(III); Theoretical Investigation on Molecular and Electronic Properties Based on the *ab initio* HF and Various DFT Methods

H. Aghabozorg[a,*], F. Manteghi[a], M. Ghadermazi[b], M. Mirzaei[c], A.R. Salimi[c] and H. Eshtiagh-Hosseini[c]

[a]*Faculty of Chemistry, Tarbiat Moallem University, Tehran, Iran*
[b]*Department of Chemistry, Faculty of Science, University of Kurdistan, Sanandaj, Iran*
[c]*Department of Chemistry, School of Sciences, Ferdowsi University of Mashhad, Mashhad, Iran*

A new compound of Sb(III), formulated as $(pipzH_2)[Sb_2(pydc)_4].2H_2O$ (**1**), was synthesized and characterized by IR, ^{1}H and ^{13}C NMR spectroscopy, elemental analysis and single crystal X-ray diffractometry. The compound (**1**) is a member of a great family of supramolecular metallic compounds recently derived from a proton transfer ion pair *i.e.* $(pipzH_2)(pydc)$, where pipz is piperazine and $pydcH_2$ is pyridine-2,6-dicarboxylic acid. In the title compound with a binuclear structure, Sb(III) atoms are pentacoordinated and the coordination polyhedra show distortion from a regular trigonal bipyramid due to stereochemically active lone pair on metallic centers. The four $(pydc)^{2-}$ ligands of the formula unit behave differently against metallic centers, *i.e.* two act as tridentate, and the other two as bidentate ligands. A variety of intermolecular O-H⋯O, N-H⋯O and C-H⋯O hydrogen bonds involving water molecules, cationic and anionic fragments are responsible for the extension of the supramolecular network of the compound. Optimized geometries were calculated for the title compound with the HF, B3LYP, B3PW91, B3P86 and B1LYP methods of theory by using the combination of LanL2DZ basis set with standard basis set 6-31G (d,p). The agreement between the optimized and experimental geometries was in the decreasing order: B3P86, B3PW91, B1LYP, B3LYP and HF. Electronic properties of the title compound were also investigated based on the natural bond orbital (NBO) analysis.

INTRODUCTION

Recently, there has been extensive interest in preparing metal-organic frameworks (MOFs) which are constructed by metal ions and organic ligands, due to their intriguing molecular topologies and potential applications in ion exchange, fluorescence, and adsorption properties [1], gas storage and separation applications as well as in catalysis, gas-sensing, and photovoltaics [2]. The primary focus of

contemporary crystal engineering, a sub-discipline of supramolecular chemistry, is the identification or design of molecular level building blocks (supramolecular synthons), whose interactions with other modular units [including self-complementary interaction(s)] exhibit some degree of predictability. In comparison to organic crystal engineering, the advantage of using metal ions in general, and transition metal ions in particular (inorganic crystal engineering), in the form of metal-ligand complexes is to introduce directional supramolecular interactions of the main coordination unit with the neighboring units and provide an opportunity to tune the

---

*Corresponding author. E-mail: aghabozorg@saba.tmu.ac.ir

nature of these interactions to novel structures of varying dimensionality and topology. The combination of coordination chemistry with noncovalent interactions, such as hydrogen bonding, provides a powerful method for creating supramolecular architectures from simple building blocks. Both types of connection are valuable for the design of network solids since they are directional interactions [3].

During the last 15 years, the crystal design and engineering of multidimensional arrays and networks have witnessed considerable progress. Chemists have learned a lot about manipulating the intermolecular forces, particularly highly directional metal ligand and hydrogen bonds, to construct supramolecular solid state architectures with interesting structures and useful properties [4]. Members of our team have put in a great deal of effort to design and synthesize such compounds with various ion pairs and metallic ions which recently have been reviewed [5]. After the synthesis of (pipzH$_2$)(pydc) as a proton transfer ion pair [6], we synthesized an extended range of compounds applying the ion pair to corresponding metallic salts such as Al(III) [7a], Mn(II) [7b], Fe(II) [7c], Co(II) [7d], Ni(II) [7e], Pd(II) [6], Cu(II) [7f], Zn(II) [7g], Cd(II) [7h], Hg(II) [7i], In(III) [7j], Tl(III) [6], Pb(II) [7k] and Bi(III) [7l]. From among the above-mentioned compounds, only Tl(III) and Bi(III) structures are similar to **1** and form binuclear structures. With other ion pairs, different binuclear Sb(III) compounds have been synthesized which will be compared in the following sections [8,9].

Recently, our team carried out the first-principle studies related to MOFs [7h] at the Hartree-Fock (HF) and density functional (DF) levels of theory. Although the synthesis, structural and spectroscopic analyses and development of applications of MOFs are extremely rich areas of research [5], relatively few high-level computational studies have been reported to reflect the intensive computational demands warranted by the large size of some of these categories of species possessing polymer-type structure. In this paper, the theoretical investigations have only been conducted on binuclear structure of Sb(III).

EXPERIMENTAL

Materials and Instrumentation

Pyridine-2,6-dicarboxylic acid (97%), piperazine (99%)

and antimony(III) chloride (99.9%) were purchased from Merck. IR spectroscopy was performed applying a Perkin-Elmer 843 spectrophotometer (200-4000 cm^{-1}) using KBr disc. NMR spectra were taken applying a Bruker DRX 500-Avance spectrometer. Chemical shifts are reported on the δ scale relative to TMS. Elemental analysis was performed with a Heraus CHN Pro apparatus. The X-ray data were obtained with a Bruker SMART Diffractometer. Melting points were determined applying a Barnstead Electrothermal 9200 apparatus.

Synthesis of (pipzH$_2$)[Sb$_2$(pydc)$_4$]·2H$_2$O

An aqueous solution of 1 mmol (228 mg) SbCl$_3$ was mixed with an aqueous solution of 2 mmol (506 mg) (pipzH$_2$)(pydc) which was prepared according to literature [6], and the total volume was 250 ml. After 2 h stirring and heating to 70-80 °C, the solution had very little precipitate that was filtered. The remaining solution was allowed to stand for two weeks. After that, colorless crystals in two types, block and needle, were obtained. The block crystals were selected for crystal structure determination. m.p.: decomp. >320°. ^{1}H NMR (D$_2$O) δ (ppm): 8.24-8.42 (m, 12H, CH, 4pydc), 3.33 (s, 8H, CH$_2$, pipzH$_2$); Anal. Calcd. for C$_{32}$H$_{28}$N$_6$O$_{18}$Sb$_2$: C, 37.38; H, 2.74; N, 8.17. Found: C, 37.58; H, 2.51; N, 8.03. Selected IR data (KBr pellet, cm^{-1}): 3600-3000 (br, stretching CH, NH and OH), 1632 and 1379 (s, COO$^-$ group), 1572 (s, scissoring NH), 1556-1426 (m, aromatic C=C), 1187 (m, stretching CN).

X-Ray Crystallography

Single crystals of the compound suitable for crystallography were selected. Unit cell determination and data of the compounds were collected on a Bruker APEX II CCD area detector system using Mo Kα radiation (λ = 0.71073 Å). The structures were solved and refined using APEX2 [10] and SHELXTL [11] program packages by full-matrix least-squares techniques on F^2. The absorption correction type was multi-scan. The H atoms of H$_2$O molecule and NH$_2$ groups were located from Fourier difference maps and refined in isotropic approximation with constrained O(N)H distance equalling 0.85(0.92) Å. Refinement of F^2 was against all reflections. The weighted R-factor, wR and goodness of fit S were based on F^2, conventional R-factors were based on F, with F set to zero for negative F^2. The threshold expression of

$F^2 > 2\sigma(F^2)$ was used only for calculating R-factors(gt) *etc.*, and was not relevant to the choice of reflections for refinement. R-factors based on F^2 were statistically about twice as large as those based on F, and R-factors based on all data would be even larger. All esds (except the esd in the dihedral angle between two l.s. planes) were estimated using the full covariance matrix. The cell esds were taken into account individually in the estimation of esds in distances, angles and torsion angles; correlations between esds in cell parameters were only used when they were defined by crystal symmetry. An approximate (isotropic) treatment of cell esds was used for estimating esds involving l.s. planes.

RESULTS AND DISCUSSION

Synthesis and Spectroscopy

The title compound was synthesized starting with (pipzH$_2$)(pydc) and corresponding metallic salt in 2:1 molar ratio, as shown in Scheme 1. As is obvious, the shifts and splittings of peaks compared to the ion pair are attributed to the presence of and coordination to the metal ion.
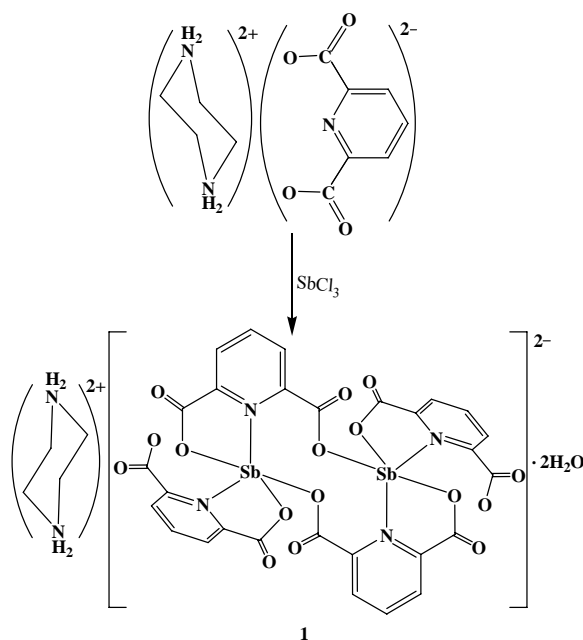
In the IR spectrum of the compound, (pipzH$_2$)[Sb$_2$ (pydc)$_4$].2H$_2$O in KBr pellet, the essential peaks are the same as the (pipzH$_2$)(pydc). The peaks of 3000-3600 cm^{-1} are attributed to stretching C-H, N-H and O-H bonds of (pipzH$_2$)$^{2+}$, (pydc)$^{2-}$ and water molecules of the lattice. Apparently, the peak at 1632 and 1379 cm^{-1} are attributed to C=O and C-O bonds of carboxylate group. The absorption peaks are the same as 1610 and 1365 cm^{-1} of the ion pair attributed to resonance of COO$^-$ group. In fact, v(C-O) and v(C=O) bands are transformed into the symmetric and antisymmetric stretching vibrations of the carboxylate anion [12] which in the complex has lost the resonance and changed to a double C=O and a single C-O bond. The sharp and strong peaks of 1572 cm^{-1} are related to scissoring NH and multiplet, medium peaks at 1556-1426 cm^{-1} are due to aromatic C=C bonds. Finally, sharp and medium absorption at 1187 cm^{-1} is attributed to stretching mode of C-N bonds.

The ^{1}H NMR spectrum of the compound in D$_2$O shows the characteristic peaks of (pydc)$^{2-}$ in 8.42-8.25 ppm, and of (pipzH$_2$)$^{2+}$ in 3.33 ppm. The peaks are similar to those of (pipzH$_2$)(pydc).

Molecular Structure

The crystallographic data of (pipzH$_2$)[Sb$_2$(pydc)$_4$].2H$_2$O are given in Table 1, the selected bond lengths and angles and

Scheme 1. The path to synthesize (pipzH$_2$)[Sb$_2$(pydc)$_4$].2H$_2$O

torsion angles are shown in Table 2 and the hydrogen bond geometry is shown in Table 3. The crystal and molecular structure of the compound, its coordination polyhedron and the crystal packing diagram are illustrated in Figs. 1, 2 and 3, respectively.

To the best of our knowledge, binuclear Sb(III) complexes are less synthesized and studied than those of binuclear Sb(V). For instance, binuclear antimony(V) complexes formulated as $Que(O_2SbPh_3.H_2O)(OSbPh_3Cl)$, $Que(OH)_3$ is quercetin [13], $Cl_3Sb(O)[R_3(R_{1O})PO_2](OR_2)SbCl_3$ with R1 = R2 = CH_3, C_2H_5 and $R_3 = C_6H_5CH_2$, $(CH_3)_3C_6H_2CH_2$ which in solution slowly exchanges the R_2 groups between the oxygen atoms of the Sb_2O_2 ring [14], along with many other Sb(V) examples [15-20]. However, binuclear Sb(III) complexes with oxo-bridged structures have been synthesized by our group including $[Sb(pydc)(H_2O)]_2O$ and $\{[Sb(pydc)(phen)]_2O\}$. $2DMSO.4H_2O$ [8,9]. In the title compound, two $(pydc)^{2-}$ ligands coordinated to each metallic center are nearly perpendicular to each other, the angle between N1/C2-C6 and N2/C9-C13 rings is 86.56°, and they act in different manners. In effect, one $(pydc)^{2-}$ acts as a tridentate ligand and the other as a bidentate ligand. It seems that this is due to steric hinderance of active lone pair

Table 1. Crystallographic Data

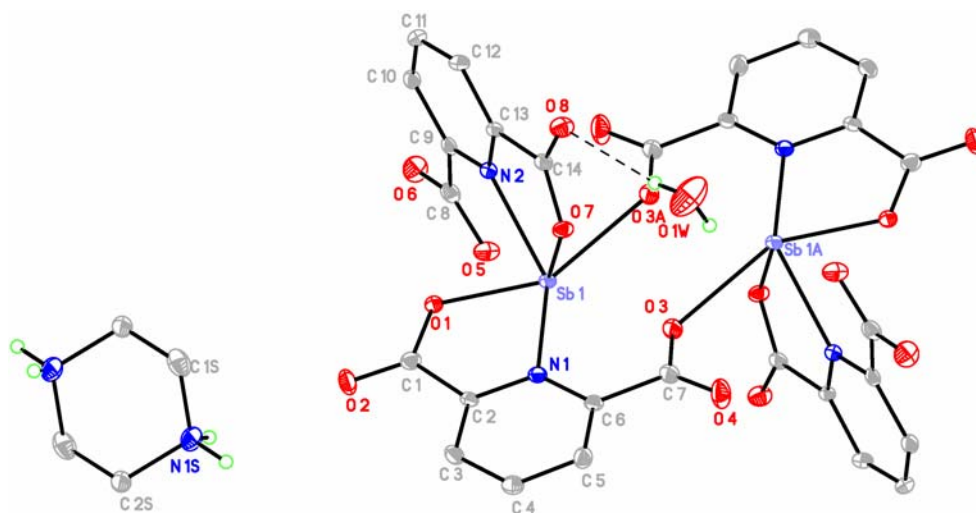|	
Formula	$Sb_2C_{28}H_{12}N_4O_{16}{}^{2-}.C_4H_{12}N_2{}^{2+}.2H_2O$
Formula weight	1028.10
Temperature	100 (2) K
Wavelength	0.71073 Å
Crystal system	Triclinic
Space group	$P\bar{1}$
Size, color and shape of crystals	0.10 × 0.10 × 0.02 mm, yellow, plate
Unit cell dimensions	
a	7.268(1) Å
b	10.574(2) Å
c	12.182(2) Å
α, β, γ	64.761(3)°, 83.563(3)°, 89.212(3)°
Volume	840.9(2) Å^3
Z	1
$D_{calc.}$	2.030 mg m^{-3}
Absorption coefficient	1.704 mm^{-1}
F(000)	508
Reflections measured	8874
Independent reflections	3984
R_{int}	0.040
Observed reflections [$I > 2\sigma(I)$]	3477
Parameters	264
Goodness-of-fit on F^2	1.025
*R*1 [$I > 2\sigma(I)$]	0.0341
*wR*2 (all data)	0.0819

Crystallographic data for the title structure has been deposited with the Cambridge Crystallographic Data Centre, CCDC 669599. Copies of the data can be obtained free of charge on application to the Director, CCDC, 12 Union Road, Cambridge CB2 1EZ, UK (Fax: int. code+ (1223)336-033; e-mail for inquiry: fileserv@ccdc.cam.ac.uk; e-mail for deposition: deposit@ccdc.cam.ac.uk).

Table 2. Selected Bond Lengths, Bond Angles and Torsion Angles (Å, °)

Sb1-O7	2.088 (2)	Sb1-N1	2.393 (3)
Sb1-O1	2.149 (2)	Sb1-O3^i	2.464 (3)
Sb1-N2	2.282 (3)		
O1-Sb1-O3^i	151.70 (9)	O3^i-Sb1-N2	77.43 (9)
O1-Sb1-N1	69.87(9)	O7-Sb1-N1	73.50 (9)
O1-Sb1-N2	74.33 (9)	O7-Sb1-N2	72.8 (1)
O3^i-Sb1-O7	76.44 (9)	O7-Sb1-O1	93.24 (9)
O3^i-Sb1-N1	129.39 (9)	N1-Sb1-N2	128.4 (1)
O7-Sb1-O1-C1	-82.9 (3)	O1-Sb1-O7-C14	-80.8 (3)

Symmetry codes: (*i*) -*x*+2, -*y*+2, -*z*+1

Table 3. Hydrogen Bond Geometry

D-H···A	D-H	H···A	D···A	D-H···A
O1W-H1WA···O5^i	0.85	2.53	3.242 (5)	142
O1W-H1WB···O7	0.85	2.58	3.304 (4)	144
O1W-H1WB···O8	0.85	2.05	2.850 (4)	156
N1S-H1SC···O1W^{ii}	0.92	1.98	2.755 (5)	141
N1S-H1SD···O6^{iii}	0.92	1.83	2.734 (5)	169
C1S-H1SA···O2	0.99	2.43	3.129 (5)	127
C1S-H1SB···O4^{ii}	0.99	2.36	3.171 (5)	139
C2S-H2SA···O4^{iv}	0.99	2.25	3.214 (5)	165
C2S-H2SB···O5^{v}	0.99	2.52	3.452 (5)	158
C12-H12A···O5^{vi}	0.95	2.46	2.980 (5)	114

Symmetry codes: (*i*) -*x*+2, -*y*+2, -*z*+1; (*ii*) -*x*+2, -*y*+1, -*z*+1; (*iii*) -*x*+1, -*y*+1, -*z*+2; (*iv*) -*x*+1, -*y*+1, -*z*+1; (*v*) *x*, *y*-1, *z*; (*vi*) *x*+1, *y*, *z*.

Fig. 1. Molecular structure of (pipzH$_2$)[Sb$_2$(pydc)$_4$].2H$_2$O at 50% probability level. Intramolecular hydrogen bond is shown with dashed lines. Symmetry code to generate equivalent atoms [A: -*x*, -*y*+2, -*z*-1].
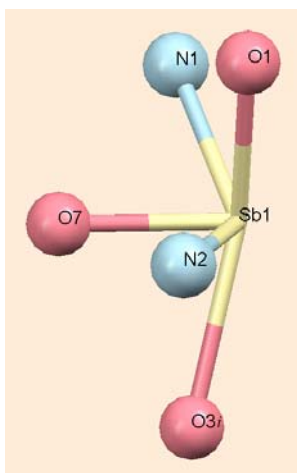
Fig. 2. Coordination polyhedron around Sb(III) atom with an empty space in one side caused by stereochemically active lone pair on metal center.
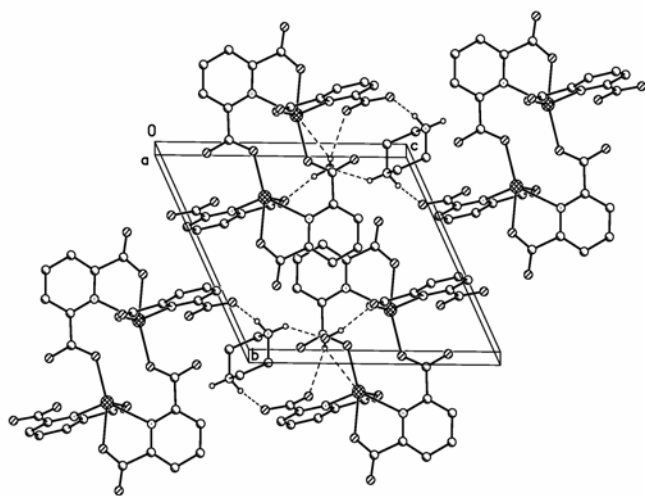

Fig. 3. Crystal packing fragment (along *a* crystal axis). Hydrogen bonds are shown as dashed lines. Only hydrogen atoms that take part in hydrogen bonding are depicted for clarity.

on Sb(III) atoms that does not allow the sixth donor atom to coordinate to the metal ion causing an empty space in the coordination sphere around five-coordinated metallic ion. We have some examples of the case, such as $(tataH_2)_2[Pb(pydc)_2]_2$.

$2tata.4H_2O$ [21] and $[Sb(pydc)(H_2O)]_2O$ [8]. The presence of active lone pair is confirmed by different bond distances around Sb(III), as shown in Fig. 1 and Table 2 of bond geometry. In fact, Sb1-O3A and Sb1-N1 bonds are obviously longer than the others, and the angles of coordination bonds around Sb(III) atom (Fig. 2) illustrate a trigonal bipyramid, with O1 and O3 lying in the axial position, which is highly distorted to a direction in the opposite side of lone pair of Sb(III).

As mentioned above, the Tl(III) [6] and Bi(III) [7l] compounds of the group are binuclear, but they are far different. In both Tl(III) and Bi(III) compounds, two metal ions are incorporated in a four-membered M_2O_2 ring, while in the title complex, the two Sb(III) atoms are members of a 10-membered ring constructed by Sb, C, N and O atoms.

Compared with the analogous compound of Bi(III), $\{(pipzH_2)[Bi_2(pydc)_4(H_2O)].H_2O\}_n$, [7l] which is in the same group as Sb(III), the Sb-O bond lengths are longer than Bi-O, while the Sb-N bond lengths are slightly shorter than Bi-N.

As shown in Table 3 and Fig. 3, various inter- and intramolecular O-H···O and N-H···O hydrogen bonds with D···A in the range of 2.734 (5) to 3.242 (5) Å and weak C-H···O hydrogen bonds with D···A in the range of 2.980 (5) to 3.452 (5) Å can be observed in crystal packing as effective factors in expanding the supramolecular network.

Computational Approach

Density functional (DF) and Hartree-Fock (HF) calculations have been done with Gaussian 98 program [22]. From among the variety of functionals, we used the following. Gradient corrections have introduced using the Becke (B) exchange [23] and the Lee, Yang, and Parr (LYP) nonlocal correlation (B1LYP) [24]. Becke's three-parameter hybrid functional, with the nonlocal correlation provided by the LYP (B3LYP) [25], Perdew 86 (B3P86) [26], and Perdew 91 (B3PW91) [27] functionals were also employed. Geometry optimizations were performed with the widely used LanL2DZ with quasi-relativistic effective core potentials (LanL2) to represent the atomic cores and double-zeta quality (DZ) to describe the valence electrons of Sb atoms with combination of standard basis set 6-31G (d,p) which is used to describe the electrons of oxygen, nitrogen, carbon, and hydrogen atoms. Electronic properties of **1** were investigated based on the

natural bond orbital (NBO) analysis, which resulted in the natural electron population and the natural charge for each atom.

Optimized Structure

The molecular structure of **1** consists of dimeric units of Sb atoms and pydc ligands. The bridging role of oxygen atoms in the complexation process, resulted in the formation of a molecular dimer which was centrosymmetric.

The optimized geometrical parameters for **1** are listed in Table 4 which also includes the experimentally determinated distances from X-ray crystallography. To facilitate the

comparison between the experimental and calculated geometrical parameters, root mean square deviation (RMSD) was calculated. For different density functional methods that were used, the accuracy of the results was improved along the following series: B3P86 (RMSD = 0.294 Å) >B3PW91 (RMSD = 0.323 Å) > B1LYP (RMSD = 0.345 Å) > B3LYP (RMSD = 0.346 Å). These results indicate that among the functionals tested, the B3P86 functional provides the most accurate geometries. The B3LYP and B1LYP geometries are close to each other, while the optimized geometry calculated by the B1LYP method is slightly better. In addition, the RMSD for all DFT methods was significantly less than the

Table 4. Comparison Between Experimental and Theoretical Bond Lengths (Å) Calculated by HF and Various DFT Methods

Geometrical parameters (Å)	Computational methods					Exp.
	HF	B3LYP	B1LYP	B3P86	B3PW91	
Sb1-N11	2.229	2.252	2.249	2.246	2.250	2.282
Sb1-N10	2.920	2.748	2.762	2.674	2.690	2.393
Sb1-O2	2.132	2.183	2.177	2.185	2.186	2.149
Sb1-O35	2.242	2.313	2.305	2.307	2.319	2.464
Sb1-O6	2.221	2.300	2.292	2.304	2.309	2.612
Sb1-O8	2.119	2.167	2.162	2.160	2.164	2.089
Sb1-Sb32	4.254	4.358	4.352	4.299	4.333	4.225
pydc#1						
C22=O6	1.265	1.288	1.286	1.282	1.283	1.254
C22=O7	1.203	1.232	1.229	1.230	1.230	1.245
C31=O8	1.274	1.300	1.298	1.295	1.296	1.293
C31=O9	1.200	1.227	1.225	1.224	1.225	1.232
C23=N11	1.314	1.332	1.331	1.328	1.329	1.330
C23=C24	1.382	1.393	1.392	1.389	1.391	1.386
pydc#2						
C12=O2	1.276	1.300	1.299	1.294	1.296	1.304
C12=O3	1.205	1.231	1.229	1.228	1.229	1.217
C21=O4	1.264	1.289	1.287	1.285	1.285	1.281
C21=O5	1.212	1.237	1.235	1.233	1.234	1.225
C20=N10	1.321	1.339	1.337	1.334	1.335	1.331
C20=C18	1.388	1.400	1.399	1.396	1.398	1.390

obtained RMSD using HF level (0.376 Å). Consequently, the agreement between calculated and experimental bond lengths has significantly been improved using DFT method.

Structural investigations on the obtained theoretical results related to the optimized structure indicate that Sb1-N1 bond length is longer than Sb1-O5 bond length with a mean of 0.45 Å at the B3LYP method. According to this evidence and the theoretical data, in the gas phase, oxygen atoms have shown higher basic properties than nitrogen atoms. Therefore, they are able to form shorter chemical bonds than nitrogen atoms with Sb atom as a Lewis acid. As an interesting feature of the present work, it should be noted that in the experimental data based upon single crystal X-ray analysis, an inverse observation was experimented of the above-mentioned theoretical results. Hence, Sb1-N1 bond length was shorter than Sb1-O5 bond length with a mean of 0.219 Å. To the best of our knowledge, the hydrogen bonding of the molecular structure plays an essential role in the observed bond length differences in theoretical and experimental studies. The typical hydrogen bond interactions namely O1W-H1WA···O5, D···A: 3.242 (5) Å, D-H···A: 142°; C2S-H2SB···O5, D···A: 3.452 (5) Å, D-H···A: 158°; C12-H12A···O5, D···A: 2.980 (5) Å, D-H···A: 114° verify the decrease in electron density and consequently the basic property of oxygen atom (O5) of carboxylate group. Accordingly, Sb atom forms stronger chemical bond with the pyridine nitrogen (N1) than with carboxylate oxygen (O5). Since, the theoretical data were obtained in the gas phase and in the absence of hydrogen bonding, in addition to the higher basic property of oxygen atom, Sb atom prefers to take oxygen electron pair rather than nitrogen atom.

Electronic Properties

The natural charges and valence configurations on the atoms of **1** were calculated using natural bond orbital (NBO) analysis based on the optimized structure in the B3LYP method (See Table 5). Regarding the charge density on the atoms and its relative relationship with basicity properties which were previously reported [28-30], here, our calculations suggest that the oxygen atoms of pydc ligands bonded to Sb atom with more natural charge are much more basic than not bonded oxygen atoms. Since the C=O (bonded) bond length is longer than C=O (not bonded) bond, it is concluded that during the complex formation, the increase of negative charge and thereupon the basic property of bonded oxygen atom render C=O bond weaker.

Furthermore, the bridging oxygen atoms between two monomers of Sb complex (O3 and O3A) with lower natural charge (-0.79) than with the other bonded oxygen atoms, as well as their longest bond lengths with Sb atoms in **1**, show

Table 5. The Natural Valence Configurations and Natural Charges on Atoms at the B3LYP Method

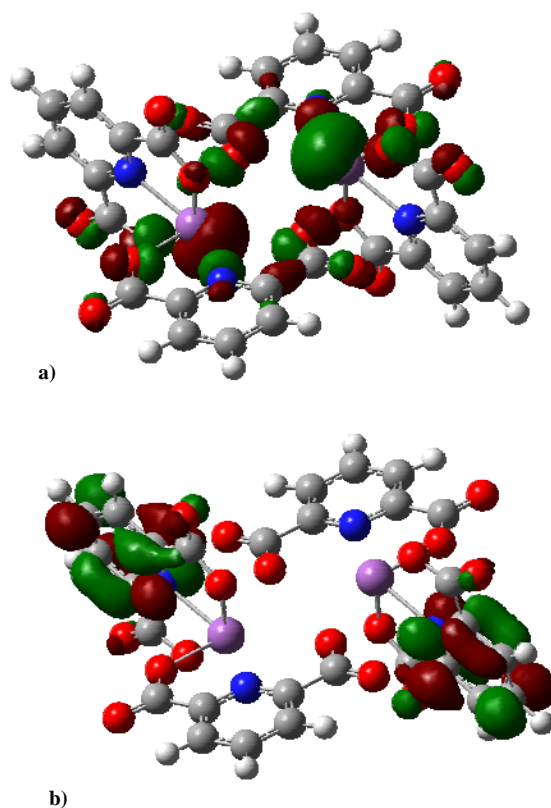| Atom	Valence configuration	Natural charge
Sb	[core]5s(1.83)5p(1.20)	1.95
pydc#1		
O6(bonded)	[core]2s(1.71)2p(5.07)	-0.79
O8(bonded)	[core]2s(1.70)2p(5.09)	-0.80
O7(free)	[core]2s(1.71)2p(4.94)	-0.67
O9(free)	[core]2s(1.71)2p(4.92)	-0.64
N11(bonded)	[core]2s(1.30)2p(4.24)	-0.56
pydc#2		
O2(bonded)	[core]2s(1.70)2p(5.12)	-0.83
O4(bonded)	[core]2s(1.70)2p(5.09)	-0.79
O3(free)	[core]2s(1.71)2p(4.94)	-0.67
O5(free)	[core]2s(1.71)2p(4.96)	-0.69
N10(bonded)	[core]2s(1.33)2p(4.11)	-0.46

Fig. 4. Schematic representation of a) HOMO and b) LUMO orbitals.

that this oxygen atom is engaged in van der Waals contact with two Sb atoms of two monomers, simultaneously. In fact, we had expected that the long bond would reproduce the bigger natural charge than its available amount, but the feasibility of interaction with two Sb atoms did not let this happen. Such evidence verifies the bridging role of the oxygen atoms.

The highest occupied molecular orbital (HOMO) and the lowest unoccupied molecular orbital (LUMO) of **1** are represented in Fig. 4. The HOMO orbital shows much more distribution of molecular orbital on Sb atom, which is attributed to the presence of lone pair. On the other hand, the LUMO orbital illustrates higher distributions of MO on pydc#1 than the other does.

CONCLUSIONS

In this paper, we have reported synthesis and crystal structure of a binuclear Sb(III) compound and the investigation of molecular structure by using the *ab initio* HF and various DFT methods. To facilitate the comparison between the experimental and calculated geometrical parameters, root mean square deviation (RMSD) was calculated. According to the obtained results, among the functionals tested, the B3P86 functional provides the most accurate geometries. In addition, the electronic properties of **1** were investigated based on the B3LYP method. The natural charges and valence configurations on the oxygen atoms indicated their low basicity and so, the longest Sb-O bond lengths. Evidence of this nature verifies the bridging role of oxygen atoms between the two monomers.

ACKNOWLEDGEMENTS

REFERENCES

[1]   F.X. Sun, G.-S. Zhu, Q.-R. Fang, S.-L. Qiu, Inorg. Chem. Commun. 10 (2007) 649.

[2]   S. Turner, O.I. Lebedev, F. Schröder, D. Esken, R.A. Fischer, G. Van Tendeloo, Chem. Mater. 20 (2008) 5622.

[3]   V. Balamurugan, J. Mukherjee, M.S. Hundal, R. Mukherjee, Struct. Chem. 18 (2007) 133.

[4]   A.M. Madalan, N. Avarvari, M. Andruh, Cryst. Growth Des. 6 (2006) 1671.

[5]   H. Aghabozorg, F. Manteghi, S. Sheshmani, J. Iran. Chem. Soc. 5 (2008) 184 and references [31-140] therein.

[6]   H. Aghabozorg, M. Ghadermazi, F. Manteghi, B. Nakhjavan, Z. Anorg. Allg. Chem. 632 (2006) 2058.

[7]   a) M. Ghadermazi, H. Aghabozorg, S. Sheshmani, Acta Crystallogr. E63 (2007) m1919; b) H. Aghabozorg, P. Ghasemikhah, J. Soleimannejad, M. Ghadermazi, J. Attar Gharamaleki, Acta Crystallogr. E62 (2006) m2266; c) H. Aghabozorg, A. Nemati, Z. Derikvand, M. Ghadermazi, Acta Crystallogr. E63 (2007) m2921; d) H. Aghabozorg, J. Attar Gharamaleki, M. Ghadermazi, P. Ghasemikhah, J. Soleimannejad, Acta Crystallogr. E63 (2007) m1803; e) H. Aghabozorg, J. Attar Gharamaleki, P. Ghasemikhah, M. Ghadermazi, J. Soleimannejad, Acta Crystallogr. E63 (2007) m1710; f) H. Aghabozorg, F. Zabihi, M. Ghadermazi, J. Attar Gharamaleki, S. Sheshmani, Acta Crystallogr. E62 (2006) m2091; g) H. Aghabozorg, M. Ghadermazi, F. Zabihi, B. Nakhjavan, J. Soleimannejad, E. Sadr-khanlou, A. Moghimi, J. Chem. Crystallogr. 38 (2008) 645; h) H. Aghabozorg, F. Manteghi, M. Ghadermazi, M. Mirzaei, A.R. Salimi, A. Shokrollahi, S. Derki, H. Eshtiagh-Hosseini, J. Mol. Struct. 919 (2009) 381; i) H. Aghabozorg, P. Ghasemikhah, M. Ghadermazi, J. Attar Gharamaleki, S. Sheshmani, Acta Crystallogr. E62 (2006) m2269; j) H. Aghabozorg, M. Ghadermazi, S. Sheshmani, B. Nakhjavan, Acta Crystallogr. E62 (2006) m2371; k) H. Aghabozorg, P. Ghasemikhah, M. Ghadermazi, S. Sheshmani, Acta Crystallogr. E62 (2006) m2835; l) H. Aghabozorg, A. Nemati, Z. Derikvand, M. Ghadermazi, Acta Crystallogr. E64 (2008) m374.

[8]   H. Aghabozorg, P. Dalir Kheirollahi, A. Moghimi, E. Sadr-khanlou, Anal. Sci. 21 (2005) x79.

[9]   H. Aghabozorg, F. Ramezanipour, B. Nakhjavan, J. Soleimannejad, J. Attar Gharamaleki, M.A. Sharif, J. Cryst. Res. Technol. 42 (2007) 1137.

[10]   Bruker, APEX II, version 2.0-1, Bruker AXS Inc., Madison, Wisconsin, USA, 2007.

[11]   G.M. Sheldrick, SHELXTL, version 5.1. Acta Crystallogr. A64 (2008) 112.

[12]   A.C. Gonzalez-Baro´, E.E. Castellano, O.E. Piro, B.S. Parajo´n-Costa, Polyhedron 24 (2005) 49.

[13]   C. Demicheli, F. Frézard, C. Malheiros, T.J. Nagem, Main Group Met. Chem. 24 (2001) 85.

[14]   H.D. Hornung, K.W. Klinkhammer, J.E. Faerber, A. Schmidt, W. Bensch, Z. Anorg. Allg. Chem. 622 (1996) 1038.

[15]   H.D. Hornung, K.W. Klinkhammer, A. Schmidt, Z. Anorg. Allg. Chem. 51 (1996) 975.

[16]   A. Burchardt, K.W. Klinkhammer, A. Schmidt, Main Group Met. Chem. 22 (1999) 301.

[17]   H.D. Hornung, K.W. Klinkhammer, A. Schmidt, Main Group Met. Chem. 20(3) (1997) 157.

[18]   M. Lauster, K.W. Klinkhammer, A. Schmidt, Main Group Met. Chem. 21 (1998) 769.

[19]   A. Burchardt, K.W. Klinkhammer, A. Schmidt, Z. Anorg. Allg. Chem. 624 (1998) 35.

[20]   G. Lang, K.W. Klinkhammer, T. Schlecht, A. Schmidt, Z. Anorg. Allg. Chem. 624 (1998) 2007.

[21]   M.A. Sharif, H. Aghabozorg, A. Shokrollahi, G. Kickelbick, A. Moghimi, M. Shamsipur, Polish J. Chem. 80 (2006) 847.

[22]   M.J. Frisch, *et al.* Gaussian 98, Revision A.7, Gaussian Inc., -Pittsburgh, PA, 1998.

[23]   A.D. Becke, Phys. Rev. A 38 (1988) 3098.

[24]   C. Lee, W. Yang, R.G. Parr, Phys. Rev. B 37 (1988) 785.

[25]   P.J. Stephens, F.J. Devlin, C.F. Chabalowski, M.J. Frisch, J. Phys. Chem. 98 (1994) 11623.

[26]   J.P. Perdew, Phys. Rev. B 33 (1986) 8822.

[27]   J.P. Perdew, Y. Wang, Phys. Rev. B 45 (1992) 13244.